Q Exam Written Report

Yubo Su
Adviser: Dong Lai

August 9, 2018

1 Introduction: White Dwarf Binaries

White Dwarfs (WDs) are commonly found in binaries in which two objects orbit their center of mass under mutual gravitational attraction. The companion object ranges from another WD to a supermassive BH (SMBH). Understanding the evolution of such systems is important to astrophysics. WD-WD binaries are most important for being thought to generate Type Ia supernovae which have been used as a "standard candle" to probe the expansion rate of the universe[14]. WD-BH systems are also interesting subjects of study. Recent works indicate that as WDs plunge close to BHs, they will produce observable flares induced by gravitational tidal forces[10]. A WD orbiting a SMBH would also produce gravitational waves that are expected to be detected by the space-based *Laser Interferometer Space Antenna (LISA)* when deployed[13]. Gravitational wave astronomy is an increasingly exciting field as the *Laser Interferometer Gravitational-Wave Observatory (LIGO)* continues to make progress since its first detection in late 2015. As gravitational wave astronomy relies on accurate predictions of the expected signals, it is important to build as accurate models as possible before observation runs begin.

1.1 Tidal Dissipation

The excitation of *internal gravity waves* (IGW) in the WD by the tidal forces of the companion is an effect exhibited in the aforementioned systems. IGWs, not to be confused with the gravitational waves above, are internal displacements in the WD fluid that oscillate and propagate due to a restoring buoyancy force. Previous work[6] indicates that IGWs can be excited in WD binaries that propagate outwards and grow exponentially due to density rarefaction, reaching nonlinear amplitudes well before the WD boundary. These waves are then expected to break and dissipate via nonlinear processes.

Previous work predicts that this dissipation mechanism can generate significantly more energy than thermal radiation from the WD surface alone and are thus a significant contribution to the WD energy budget[7]. The exact radial dissipation profile is of interest since it both is sensitive to WD properties and can produce vastly different observable outcomes. One proposed outcome is a *tidal nova*, in which heating in the WD's degenerate hydrogen layer is sufficient to trigger runaway nuclear fusion and an observable surface explosion[8]. Understanding whether such phenomena occur requires understanding how energy and angular momentum are redistributed internally inside the WD.

Internal gravity wave breaking is a nonlinear hydrodynamic phenomenon. Such phenomena are known to require numerical simulation to study in detail.

2 Work Accomplished: Theory and Numerics

To begin our numerical study of IGW breaking, we first considered 2D IGW breaking in a plane-parallel, uniformly stratified, incompressible atmosphere. Even in this reduced problem, we encountered numerous difficulties and efforts to surmount them are ongoing. Thus the subsequent two sections on the theory and

numerics of IGW breaking largely focus on the toy problem with only brief references to extensions to the full 3D, compressible problem we wish to eventually study.

2.1 IGW Theory

2.1.1 IGW System and Linear Theory

We briefly recap the studied IGW system in detail and its solution in linear theory. An incompressible 2D hydrodynamical system can be described by just four Eulerian dynamical variables ρ, P, u_x, u_z, the density, pressure and x,z components of Eulerian velocity respectively, each of which is a function of x,z,t. We notate $\rho = \rho_0 + \rho_1$ where ρ_0 is the background density satisfying hydrostatic equilibrium in the absence of any IGW and ρ_1 is the deviation that represents the IGW flow, and likewise for the remaining variables. In the linear theory, we assume $\rho_1 \ll \rho_0, P_1 \ll P_0$, and to further simplify the problem we take $u_{0x} = u_{0z} = 0$. The resulting system of equations describing IGW propagation are:

$$\vec{\nabla} \cdot \vec{u}_1 = 0, \tag{1a}$$

$$\frac{\mathrm{d}\rho_1}{\mathrm{d}t} + u_{1z}\frac{\partial \rho_0}{\partial z} = 0, \tag{1b}$$

$$\frac{\mathrm{d}\vec{u}_1}{\mathrm{d}t} + \frac{\vec{\nabla} P_1}{\rho_0} - \rho_1 \frac{\vec{\nabla} P_0}{\rho_0^2} = 0. \tag{1c}$$

In the linearized system, $\frac{\mathrm{d}}{\mathrm{d}t} = \frac{\partial}{\partial t} + \vec{u}\cdot\vec{\nabla} \approx \frac{\partial}{\partial t}$. Uniform stratification takes the form $-\frac{\partial \ln \rho_0}{\partial z} = -\frac{\partial \ln P_0}{\partial z} = H$ where H is some characteristic scale height, then it can be shown the IGW solution takes on form

$$u_{1z}(x,z,t) = A e^{z/2H} e^{i(k_x x + k_z z - \omega(k_x,k_z)t)}, \tag{2}$$

$$\omega(k_x,k_z) = \frac{N k_x}{\sqrt{k_x^2 + k_z^2 + \frac{1}{4H^2}}}, \tag{3}$$

where $N^2 = \frac{g}{H}$ the Brunt-Väisälä frequency is constant. Note the $u_{1z} \propto e^{z/2H}$ growth induced by the density stratification, and so we expect nonlinear effects to become important as $Ae^{z/2H} \sim 1$.

2.1.2 Nonlinear IGW Theory

The leading-order nonlinearities in Eq. 1 causing the plane wave solution Eq. 2 to break down are thoroughly studied in atmospheric sciences e.g.[3][2], though a verdict on the exact breaking phenomenon is still unclear. The primary two mechanisms considered by the community are:

Modulational Instability By arguments similar to those underlying Stokes Flow (the mean motion of particles in a plane wave flow), it can be shown that the plane wave solution Eq. 2 induces a mean flow $\mathcal{O}(A^2)$. Since, in the incompressible system, $\vec{k}\cdot\vec{u} = 0$ (where $\vec{k} = k_x\hat{x} + k_z\hat{z}$ is the wave vector), many of the advective terms $\vec{u}\cdot\vec{\nabla}$ vanish to second order $\vec{u}_1\cdot\vec{\nabla}\vec{u}_1 = 0$, and so the first nonlinear term to appear must be the interaction of the plane wave with its own induced mean flow.

With some algebraic manipulations, Eq. 1 can be recast in the form of a nonlinear Schrödinger Equation, whose form is $iA_t = \alpha A_{xx} + \beta|A|^2 A$. A happens here to be the complex amplitude of the Eulerian displacement, and $|A|^2$ is the mean flow term.

The weakly nonlinear Schrödinger equation can be examined for *modulational instability* by considering the evolution of modes near the propagating plane wave, i.e. a wave train centered on $\vec{k}_0$. A brief derivation of the criterion is provided in [18] and applied in [3]. The calculations show that for certain values of $\vec{k}$, the wave propagates with a weakly split group velocity that acts to reduce the amplitude and delay breaking, while for other values the group velocity is complex and exhibits

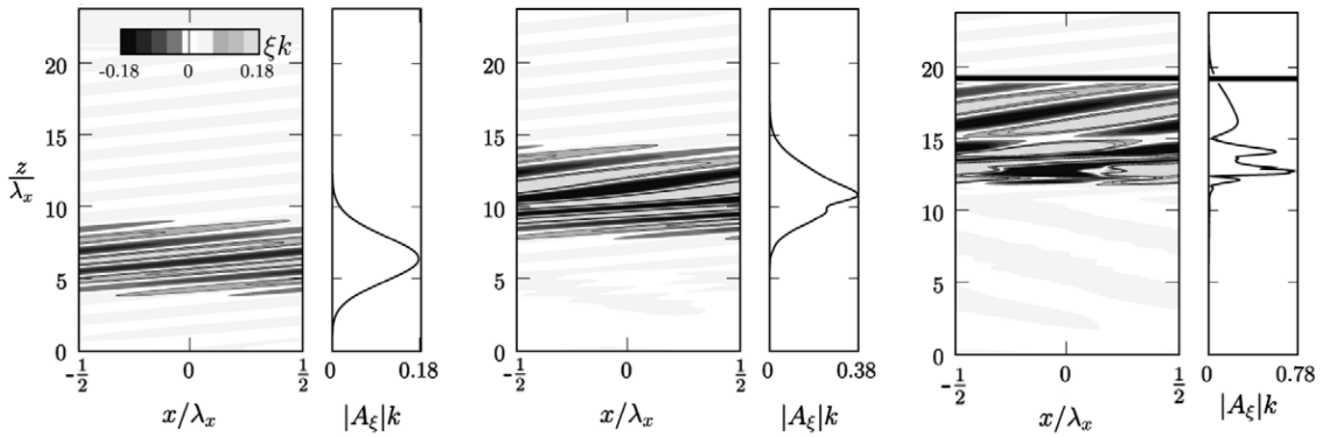

(a) $t = 100/N^{-1}$. (b) $t = 175/N^{-1}$. (c) $t = 250/N^{-1}$.

Figure 1: Modulationally unstable wavepacket breaking before the height predicted by linear theory (thick black line).

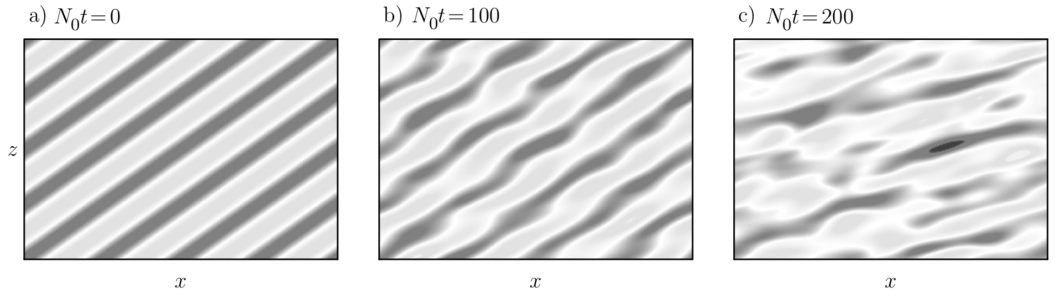

Figure 2: Breakdown of plane wave via parametric subharmonic instability. Doubly periodic boundary conditions, courtesy of [16].

breaking at lower amplitudes. An exmaple of a modulationally unstable Gaussian wavepacket is shown in Fig. 1.

Parametric Subharmonic Instability If a triad of modes with wavevectors $\vec{k}_1, \vec{k}_2, \vec{k}_3$ satisfies the triad resonance condition

$$\vec{k}_1 = \vec{k}_2 + \vec{k}_3 \qquad\qquad \omega(\vec{k}_1) = \omega(\vec{k}_2) + \omega(\vec{k}_3), \tag{4}$$

then it is possible in the nonlinear advective term $\vec{u} \cdot \vec{\nabla}$ for two modes to have a frequency component that drives the third. A careful albeit tedious derivation for the growth rate of two infinitesimal modes in the presence of a third mode such that the three satisfy Eq. 4 is given in [1]. Further Floquet analysis, as done in [4], illustrates that this produces cascades to integer multiples of the plane wave wavevector and fractions of the temporal frequency.

It bears noting that, as this is a parametric resonance, the growth of the subharmonics grows exponentially from a nonzero initial value. An example of the development of these higher modes is given in Fig. 2.

While a thorough understanding of the nonlinear theory is not strictly necessary to run simulations, it is important to be able to identify whether deviations from the linear solution in simulations are numerical artifacts or real physical effects.

2.2 Numerical Simulations

2.2.1 Choice of Software

For numerical simulations we use the spectral PDE solver `Dedalus`[12]. A number of concerns motivated our choice of software:

- Though we expect the problem to develop fine scale structure at later times, no shocks develop. Spectral methods exhibit exponential convergence when dynamical variables vary smoothly[15], and so we are able to capture better numerical precision for the same computational cost.
- As the key focus of our study is how energy cascades into smaller length scales but we have limited spatial resolution, we must introduce some nonphysical regularization at small length scales to prevent them from accumulating energy. This usually comes in the form of viscosity, so having precise control over the viscosity is necessary to understand the regime of validity of our results. Spectral methods have no numerical viscosity[15] and so allow for much more precise control over regularization.
- `Dedalus` is an exceptionally easy to use code and remains under active development. It also comes parallelized and has been extended to 3D geometries as well (although still in development).

Note however that `Dedalus`, being a fully spectral solver, does not support numerical techniques such as adaptive mesh refinement and so must use a uniform resolution throughout the simulation domain. It is thus prudent to choose a simulation subject that maximizes usage of the domain with interesting behavior.

2.2.2 Setup

Note that the objective only requires simulating IGWs near the end of their propagation, after an infinitesimal displacement has already grown to near-nonlinear amplitudes. Focusing on the end of their evolution is a tremendous computational savings both in temporal evolution and spatial resolution as discussed above.

We discuss the simulation setup and its various considerations below:

Domain We choose a 2D domain with periodic boundary conditions in the x direction and aperiodic boundary conditions in the z direction to permit density stratification. In conjunction with the damping zones below, this mimics a 2D infinite plane geometry. The choice of spectral basis functions is then Fourier in the x and Chebyshev in the z.

We want a z domain of a many scale heights to induce growth to nonlinear amplitudes, so we use $z \in [0, 10H]$. To use a similarly sized domain, we use $x \in [0, 4H]$.

We are able to use 1024 Chebyshev modes and 256 Fourier modes (memory and computation resource limited), meaning we can resolve length scales $\sim H/100$, plenty for our target $k_z = \frac{20}{H}$.

Damping Zones In order to mimic an unbounded domain in the z, we must ensure that the boundaries do not produce reflections. Such radiative boundary conditions (also outgoing/Sommerfield/absorbing boundary conditions) can only be approximate when applied to many $\vec{k}$ incoming waves[5][17].

Instead, we implement *damping zones* modeled after those used in [11]. We introduce a field $\Gamma(z)$ such that $\frac{\partial}{\partial t} \to \frac{\partial}{\partial t} + \Gamma(z)$, so that dynamical variables dissipate where Γ is nonzero. Choosing then Γ to vanish everywhere but near the boundaries suppresses reflection. In order to ensure $\Gamma(z)$ has an exponentially convergent spectral representation, we must choose smooth $\Gamma(z)$, and a traditional choice is (let $z \in [0, L_z]$ be the simulation domain)

$$\Gamma(z) = \frac{\Gamma_0}{2}\left[2 + \tanh\gamma\frac{z - z_t}{L_z - z_t} + \tanh\gamma\frac{z_b - z}{z_b}\right]. \tag{5}$$

This function is approximately zero $z \in [z_b, z_t]$ and approximately 1 in the damping zones. Furthermore, its steepness can be tuned via the parameter γ (it cannot be so steep as to run up against spatial resolution, however), and the damping timescale can be tuned by Γ_0.

In our simulation, $z_b = 0.07L_z, z_t = 0.93L_z, \gamma = 3$ and we choose $\Gamma_0 = N$ such that, in the damping zone oscillations damp on the timescale of N^{-1}.

Forcing Since we only wish to model the later stages of IGW evolution, we need only excite an IGW in the linear regime with any mechanism rather than specifically the tidal mechanism describe in the introduction.

Because Chebyshev polynomials (which satisfy $T_n(x) = \cos(n \arccos x)$) have spacing between zeros scaling as n^{-1} on the interior of the domain but cluster as n^{-2} near the edge of the domain, the effective Courant-Friedrichs-Levy condition is much stricter when spectral features exist near the edge of the domain[9].

Instead, we again follow [11] in using a volumetric forcing term to generate a plane wave IGW. We choose a forcing profile of form

$$F(x,z,t) = F_0 e^{-\frac{(z-z_0)^2}{2\sigma^2}} e^{i(k_x x - \omega_0 t)}. \tag{6}$$

If σ is chosen to be sufficiently small, then $F(x,z,t)$ will have a reasonably large component along the k_z wavevector satisfying $\omega(k_x,k_z) = \omega_0$ where $\omega(k_x,k_z)$ is the IGW dispersion relation. Thus we are able to drive on resonance and generate IGW propagating in both directions from z_0. Lastly, if we choose z_0 near the bottom of the domain, the upward propagating wave is exactly what we wish to study and the downward propagating wave is damped by the damping zone.

Since our equations of motion require the velocity to be divergence-free, we instead attach the driving term to the *density equation*. While this is ill-justifiable physically, corresponding to violating the conservation of mass periodically, it suffices for the application at hand. Thus, we use continuity equation

$$\frac{\mathrm{d}\rho_1}{\mathrm{d}t} - \rho_0 \frac{u_{1z}}{H} + \Gamma(z)\rho_1 = F_0 e^{-\frac{(z-z_0)^2}{2\sigma^2}} \cos(k_x x - \omega_0 t). \tag{7}$$

It is not so hard to compute the excited $u_{1z}(z = z_0)$ for such a forcing profile: solving for a forcing $F(x,z,t) = F_0 \delta(z - z_0) e^{i(k_x x - \omega_0 t)}$ is a simple matter of matching homogeneous solutions, then an approximation that the Gaussian excites a $e^{-k_z^2\sigma^2/2}$ smaller wave is a serviceable approximation. This gives

$$|u_{1z}(z = z_0)| = \frac{F_0\sqrt{2\pi}\sigma g k_x^2}{2\rho_0(z = z_0)\omega^2 k_z} e^{-k_z^2\sigma^2/2}. \tag{8}$$

In order for the above approximation to hold, σ must be small, so that the forcing is broad in spatial frequencies. We choose $\sigma k_z = 1$. We also use $z_0 = 0.25L_z$, so $0.1L_z$ separated from the damping zone, and we choose F_0 depending on the $u_{1z}(z = z_0)$ desired (often 0.01).

Timestepping The primary timestep that must be resolved for IGW is N^{-1} the buoyancy timescale (in IGW, $k_x \ll k_z$ and so $\omega \ll N$), so we have been testing with timesteps $\Delta t = 0.02N^{-1}$. Other simulations use a variety of timesteps $\Delta t \in [0.0025N^{-1}, 0.08N^{-1}]$ e.g. [11], [3]. Because Dedalus uses implicit timestepping for linear terms, an overly large timestep induces amplitude loss during propagation; the proper diagnostic for timestep size is ensuring $e^{z/2H}$ growth in the linear regime.

Viscosity This is the current stage of our work and is not yet well-characterized. Viscosity serves to regularize the system and drain energy preferentially from high k_z modes. In order to maintain exponential convergence, we need to ensure that any mode that excites modes beyond the scope of

our spectral expansion must be viscously damped. Thus, our regularization should damp the upper half of spectral modes.

There are two choices for implementing such viscous regularization that we are currently investigating:

Navier-Stokes Viscosity This is the traditional Navier-Stokes viscosity, which modifies the momentum equation of Eq. 1 as

$$\frac{\mathrm{d}\vec{u}_1}{\mathrm{d}t} + \frac{\vec{\nabla}P_1}{\rho_0} + \frac{\rho_1\vec{g}}{\rho_0} + \Gamma\vec{u}_1 - \nu\nabla^2\vec{u}_1 = 0. \tag{9}$$

Using our (rather heuristic) argument that half of modes should be damped in the nonlinear regime $u_1 \sim \frac{\omega}{k_z}$ then we need $\nu \sim \omega\left(\frac{L_z}{\pi N_Z}\right)^2$ where N_Z is the number of z modes. Note that $k_x \ll k_z$ does not factor into the $\nu\nabla^2$ size calculation.

Hyperviscosity Much more of a numerical trick, *hyperviscosity* refers to a family of stronger-than-Navier-Stokes viscosities. The one we consider is reaching directly into the k_z spectral coefficients and artificially decreasing those beyond $N_Z/2$. Conventionally, hyperviscosity sets these directly to zero but this seems to be too strong by our tests. Because results are still pending, the exact hyperviscosity procedure is yet to be determined.

Gradual Forcing One last trick that we are considering is to turn on the forcing term gradually; Fig. 3 shows many examples where ringing from turning the forcing term on immediately excites ringing that generates spurious nonlinear interactions. We choose to effect this by $F(t)\tanh 10\omega_0 t$, so over the course of about twenty periods the forcing will reach full amplitude. Results are pending.

N^{-1} is the unit of time and H the unit of distance in our computations, both of which are set to 1. Some snapshots from our simulation can be seen in Fig. 3. Note the smooth

3 Future Work

Mercifully omitted from this writeup are all of the misguided efforts that were slowly revised out over time. Nevertheless, against all odds we find ourselves very near conquering the 2D toy problem, with a few remaining difficulties to be elaborated below.

3.1 Remaining 2D Work

We are very close to having a full working simulation of 2D wave breaking without numerical singularities. The largest further obstacle that stands in our way is computational expense, which is being rectified presently within the group. Compounding our difficulties are that, in the $k_x \ll k_z$ limit that most astrophysical IGWs find themselves in, the group velocity is extremely slow, and so requiring resolving N^{-1} timescales results in a very slow simulation. Even so, we should soon understand where the dissipation in these excited IGWs occurs as they break via nonlinear processes.

3.2 3D Work

`Dedalus` has been adapted for 3D work, using spherical harmonics and Chebyshev polynomials, so the software package is sufficiently up-to-date for our problem. Nevertheless, 3D calculations will be even more expensive and will likely carry with them another host of instabilities to sort out. Armed with our understanding of these 2D difficulties, however, it should be much easier to tackle.

We also intend to extend our 3D calculations to realstic WD equations of state and density profiles[6], such as those in Fig. 4. These will all have to be adapted somewhat to fit the requirements of `Dedalus`. .

4 Conclusion and Acknowledgements

In conclusion, we are very close to a numerical solution to the 2D plane parallel atmosphere IGW breaking problem, with only a few more kinks to sort out. With this, we should be able to interpret our results within the framework of existing theory and, after having understood this thoroughly, generalize our approach to the full realistic 3D problem.

I would like to thank Professor Dong Lai for advising me both as a lab member and as a first year graduate student during the past year. I would also like to thank Daniel Lecoanet for explaining his unending back of numerical tricks for using `Dedalus` to me.

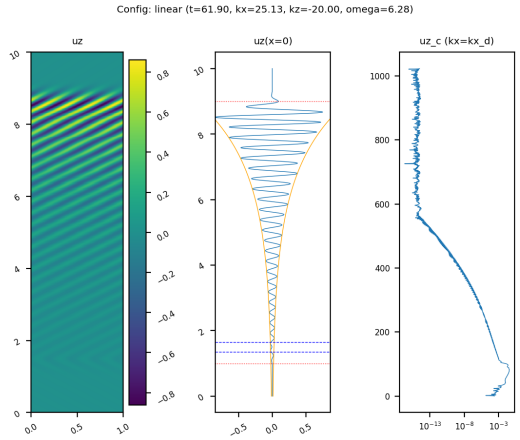

(a) Linear simulation. Note the close agreement of the analytically predicted excitement amplitude and the actual waveform. The spectrum is broader than a pure Fourier spectrum due to the waveforms being sinusoidal and the basis being Chebyshev.

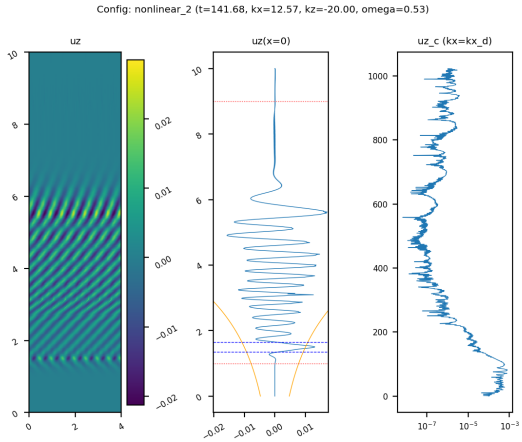

(b) Nonlinear simulation without regularization. The mismatch of the analytical envelope is not significant. Note the significant amplitude in higher Chebyshev modes. The simulation breaks soon after this point, seemingly due to parametric subharmonic instability.

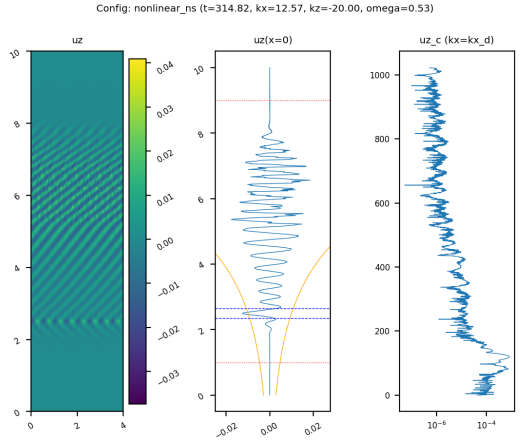

(c) Nonlinear simulation with Navier-Stokes regularization. The mismatch of the analytical envelope is again not significant. The supposed PSI from the non-regularized system is clearly just ringing from starting the forcing in discontinuous fashion.

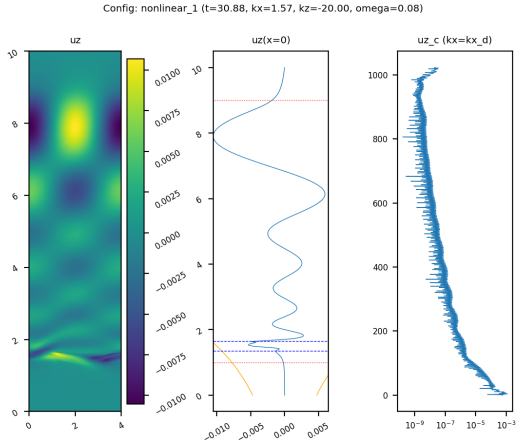

(d) Another consequence of starting the forcing in discontinuous fashion, nonlinear terms amplify the waveform in the driving zone and produces nonphysical shocks.

Figure 3: The four simulation snapshots above include the following notation: the left plot is a simple 2D plot of the $u_{1z}(x,z)$ field, the middle plot is a slice $u_{1z}(x=0,z)$ and the right plot plots the Chebyshev spectral expansion at the driving k_x. In the middle plots, the two dashed red lines indicate the damping zones, the dashed blue lines indicate the forcing zone $\pm 3\sigma$ and the orange solid lines indicate the analytically predicted envelope.

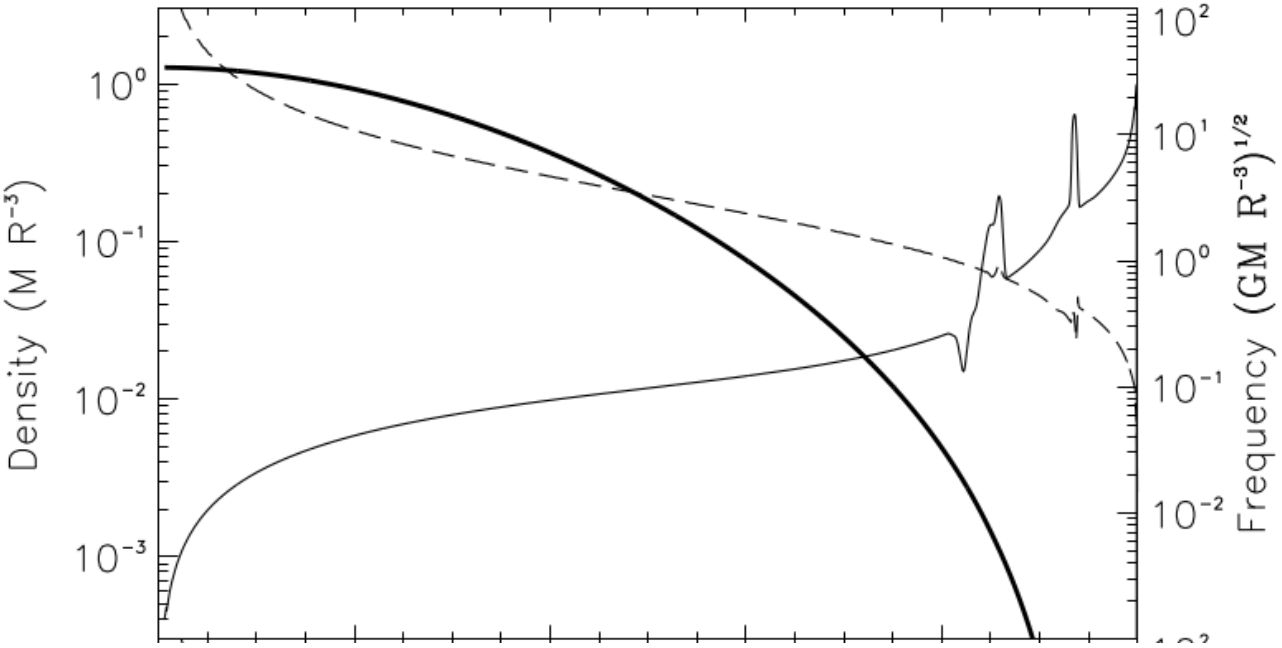

Figure 4: Dynamical variables for a realistic WD model. The thick line is the density and the thin line is N^2. The dashed line is the square of the Lamb frequency, not discussed in this paper but important to 3D waves.

References

[1] Baptiste Bourget, Thierry Dauxois, Sylvain Joubaud, and Philippe Odier. Experimental study of parametric subharmonic instability for internal plane waves. *Journal of Fluid Mechanics*, 723:1–20, 2013. doi: 10.1017/jfm.2013.78.

[2] Hayley V. Dosser and Bruce R. Sutherland. Anelastic internal wave packet evolution and stability. *Journal of the Atmospheric Sciences*, 68 (12):2844–2859, 2011. doi: 10.1175/JAS-D-11-097.1. URL https://doi.org/10.1175/JAS-D-11-097.1.

[3] H.V. Dosser and B.R. Sutherland. Weakly nonlinear non-boussinesq internal gravity wavepackets. *Physica D: Nonlinear Phenomena*, 240 (3):346 – 356, 2011. ISSN 0167-2789. doi: https://doi.org/10.1016/j.physd.2010.09.008. URL http://www.sciencedirect.com/science/article/pii/S0167278910002587.

[4] Philip G. Drazin. On the instability of an internal gravity wave. *Proceedings of the Royal Society of London A: Mathematical, Physical and Engineering Sciences*, 356(1686):411–432, 1977. ISSN 0080-4630. doi: 10.1098/rspa.1977.0142. URL http://rspa.royalsocietypublishing.org/content/356/1686/411.

[5] Bjorn Engquist and Andrew Majda. Radiation boundary conditions for acoustic and elastic wave calculations. *Communications on Pure and Applied Mathematics*, 32(3):313–357, 1979. doi: 10.1002/cpa.3160320303. URL https://onlinelibrary.wiley.com/doi/abs/10.1002/cpa.3160320303.

[6] Jim Fuller and Dong Lai. Tidal excitations of oscillation modes in compact white dwarf binaries – i. linear theory. *Monthly Notices of the Royal Astronomical Society*, 412(2):1331–1340, 2011. doi: 10.1111/j.1365-2966.2010.18017.x. URL http://dx.doi.org/10.1111/j.1365-2966.2010.18017.x.

[7] Jim Fuller and Dong Lai. Dynamical tides in compact white dwarf binaries: tidal synchronization and dissipation. *Monthly Notices of the Royal Astronomical Society*, 421(1):426–445, 2012. doi: 10.1111/j.1365-2966.2011.20320.x. URL +http://dx.doi.org/10.1111/j.1365-2966.2011.20320.x.

[8] Jim Fuller and Dong Lai. Tidal novae in compact binary white dwarfs. *The Astrophysical Journal Letters*, 756(1):L17, 2012. URL http://stacks.iop.org/2041-8205/756/i=1/a=L17.

[9] David Gottlieb and Eitan Tadmor. The cfl condition for spectral approximations to hyperbolic initial-boundary value problems. *Mathematics of Computation*, 56(194):565–588, 1991.

[10] Jamie Law-Smith, Morgan MacLeod, James Guillochon, Phillip Macias, and Enrico Ramirez-Ruiz. Low-mass white dwarfs with hydrogen envelopes as a missing link in the tidal disruption menu. *The Astrophysical Journal*, 841(2):132, 2017. URL http://stacks.iop.org/0004-637X/841/i=2/a=132.

[11] D. Lecoanet, G. M. Vasil, J. Fuller, M. Cantiello, and K. J. Burns. Conversion of internal gravity waves into magnetic waves. *Monthly Notices of the Royal Astronomical Society*, 466(2):2181–2193, 2017. doi: 10.1093/mnras/stw3273. URL http://dx.doi.org/10.1093/mnras/stw3273.

[12] Daniel Lecoanet, Michael Le Bars, Keaton J. Burns, Geoffrey M. Vasil, Benjamin P. Brown, Eliot Quataert, and Jeffrey S. Oishi. Numerical simulations of internal wave generation by convection in water. *Phys. Rev. E*, 91:063016, Jun 2015. doi: 10.1103/PhysRevE.91.063016. URL https://link.aps.org/doi/10.1103/PhysRevE.91.063016.

[13] Gijs Nelemans. The galactic gravitational wave foreground. *Classical and Quantum Gravity*, 26(9):094030, 2009. URL http://stacks.iop.org/0264-9381/26/i=9/a=094030.

[14] S. Perlmutter, G. Aldering, G. Goldhaber, R. A. Knop, P. Nugent, P. G. Castro, S. Deustua, S. Fabbro, A. Goobar, D. E. Groom, I. M. Hook, A. G. Kim, M. Y. Kim, J. C. Lee, N. J. Nunes, R. Pain, C. R. Pennypacker, R. Quimby, C. Lidman, R. S. Ellis, M. Irwin, R. G. McMahon, P. Ruiz-Lapuente, N. Walton, B. Schaefer, B. J. Boyle, A. V. Filippenko, T. Matheson, A. S. Fruchter, N. Panagia, H. J. M. Newberg, W. J. Couch, and The Supernova Cosmology Project. Measurements of nd rom 42 high-redshift supernovae. *The Astrophysical Journal*, 517(2):565, 1999. URL http://stacks.iop.org/0004-637X/517/i=2/a=565.

[15] William H Press, Saul A Teukolsky, William T Vetterling, and Brian P Flannery. *Numerical recipes 3rd edition: The art of scientific computing*. Cambridge university press, 2007.

[16] Bruce R Sutherland. *Internal gravity waves*. Cambridge university press, 2010.

[17] Ludwig Wagatha. Approximation of pseudodifferential operators in absorbing boundary conditions for hyperbolic equations. *Numerische Mathematik*, 42(1), Mar 1983. ISSN 0945-3245. doi: 10.1007/BF01400917. URL https://doi.org/10.1007/BF01400917.

[18] Gerald Beresford Whitham. *Linear and nonlinear waves*, volume 42. John Wiley & Sons, 2011.